ROBOT NAVIGATION USING A PRESSURE GENERATED MECHANICAL STRESS FIELD "THE BIHARMONIC POTENTIAL APPROACH"

BY

Ahmad A. Masoud†, Samer A. Masoud‡, Mohamed M. Bayoumi†

† Robotics Laboratory
Electrical Engineering Department, Queen's University,
Kingston, Ontario, Canada K7L-3N6.

‡ Department of Mechanical, Industrial, and Nuclear Engineering
College of Engineering, University of Cincinnati,
Cincinnati, Ohio, 45221-0072, USA.

ABSTRACT

This paper suggests a new approach for navigation in a known environment. The approach is based on the Biharmonic potential fields which govern mechanical stress fields in homogeneous solids. It is observed that a path generated by such a technique is free of sharp turns that may appear in its counterpart that is generated from an underlying Harmonic potential. This in turns makes a path from the former more dynamically suitable for traversal. Also, the navigation field is extracted from the Biharmonic potential in a manner that bypass the rapidly vanishing field problem which is encountered in the Harmonic potential approach. Development of the Biharmonic approach, simulation results, as well as comparison with the Neumann and Dirichlet setting of the Harmonic approach are provided.

I. INTRODUCTION

In the mid eighties several papers addressing the path planning problem [1,2,3] signaled a major departure from the traditional geometric approach for navigation. The idea of potential fields was suggested. In this approach the flow lines of a vector field that is generated from an underlying potential field (V) is used to *safely guide motion to its unique equilibrium* point which is situated on the target. The usefulness of such an idea critically hinges on the ability to find a mapping that would accept information about the target and the environment as an input and generate a field that spans the whole workspace of interest. This field has to be locally usable in an a priori specified manner that is independent of the starting point to safely direct motion to the target. The mapping can be seen as a tool for fanning the operator's control over *the workspace. With such a mapping a small (seed) space* can be used to generate a field that spans a much larger space (both in volume and dimensionality) that is in turn usable for inducing the behavior of interest. Of course, it is possible to construct such a field by properly assigning a vector quantity (to tell a vehicle in which direction to proceed) to sufficient points in the workspace (an interpolation scheme may be used to fill in between the points); however, the effort in doing so is enormous. In the field synthesis process the information about the goal, the environment structure, and the desired behavior are imbedded (encoded) in the fabric of the potential in the form of locally extractable vector feature/s that are designed to operate in a chain-like manner to establish a desired global behavior through a series of local actions. Those vector features and the scheme that utilizes them to lay a path to the target are given the name TRACKING MECHANISM (we also contemplated the name STEERING MECHANISM). The vector features are extracted from the potential field by operating on it with a reflexive operator. Usually the Del (∇) operator is used to generate the gradient flow of the field (∇V). In a recent work [4,5] the use of the curl operator (∇x) in addition to ∇ was suggested to generate the navigation field. It ought to be mentioned that the tracking mechanism need not operate in a purely reflexive manner. It can be shown by examples that cognitive aspects can be integrated in the process to efficiently deal with uncertain situations and to enhance the reliability of the process. From the above discussion it can be seen that a potential-based navigation technique can be divided into two interactive stages. A stage to generate the field, and a stage to utilize that field for navigation. Figure-1 shows a block diagram of the suggested structure for such techniques.

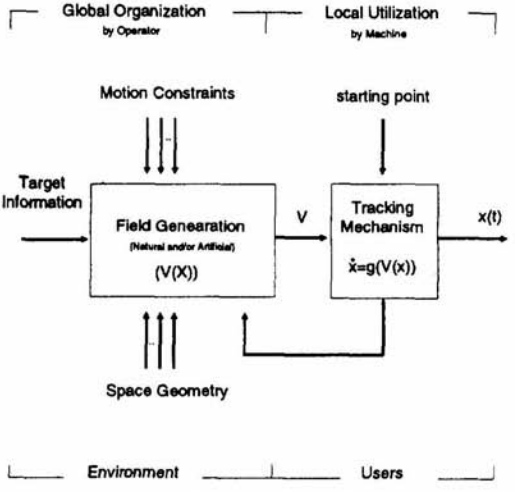

Figure 1: Basic Structure of Potential-Based. Path planning techniques.

This paper suggests a new mapping of the type that is discussed above to transform the geometry of the work space and the location of the target into a potential field that is usable for navigation. The proposed mapping makes use of the Biharmonic potential fields, which are known for mechanical engineers to govern the stress inside a homogeneous solid. Although, many potential-based techniques were proposed for navigation we choose to compare the new approach with the Harmonic potential approach [4,5,6,7,8,9,10]. Such

an approach is known to efficiently guide motion in a complex environment. The comparison takes into consideration the nature of the path that is generated by both techniques, and the computability of the navigation field.

The paper is organized as follows: In section II the Mechanical stress field theory is used to develop the Biharmonic approach. Also, the boundary value problem that generates the potential field, and the tracking mechanism are supplied. In section III simulation results and comparisons with the Harmonic potential approach are provided. Conclusions are placed in section IV.

II. THE BIHARMONIC POTENTIAL APPROACH

In this section the development of the Biharmonic potential approach is briefly presented from the point of view of mechanical stress theory. The mechanical setting that is used to derive the boundary value problem (BVP) which generates the potential is provided. And a scheme for generating the navigation field from that potential is discussed.

Mechanical Stress in Homogeneous Solids

With no loss of generality the treatment here is restricted to the 2-D case (plain stress). The treatment of the 3-D case can be found in any standard text about elasticity or continuum mechanics [11,12,13].

An infinitesimal element in a solid (Figure 2a) is subjected to a force per unit area normal to its boundary (stress). If such a force points outward the element (tension, σ_{xx}) it is considered positive; otherwise, it is negative (compression, σ_{yy}). The element is also subjected to a force per unit area that is tangent to its surface (shear) that act as a couple. If such a couple rotate c.w. they are assigned a positive value (σ_{yx}). If the rotation is c.c.w. they are considered negative (σ_{xy}). For such forces to exist in a solid they must satisfy the following relations:

1. Equilibrium of motion (no translation)

$$\frac{\partial\sigma_{xx}}{\partial x} + \frac{\partial\sigma_{xy}}{\partial y} = 0, \qquad \frac{\partial\sigma_{yx}}{\partial x} + \frac{\partial\sigma_{yy}}{\partial y} = 0. \tag{1}$$

2. Zero body moment (no rotation)

$$\sigma_{xy} = \sigma_{yx} \tag{2}$$

3. Hook's Law

This law relates the elastic deformation experienced by the element in both the x direction (u(x,y), and the y direction (v(x,y)) to the stress and the shear on that element

$$\sigma_{xy} = G\left[\frac{\partial u(x,y)}{\partial y} + \frac{\partial v(x,y)}{\partial x}\right]$$
$$\sigma_{xx} = \lambda\left[\frac{\partial u(x,y)}{\partial x} + \frac{\partial v(x,y)}{\partial y}\right] + 2G\left[\frac{\partial u(x,y)}{\partial x}\right] \tag{3}$$
$$\sigma_{yy} = \lambda\left[\frac{\partial u(x,y)}{\partial x} + \frac{\partial v(x,y)}{\partial y}\right] + 2G\left[\frac{\partial v(x,y)}{\partial y}\right].$$

Where $\lambda=\upsilon\cdot E/(1-\upsilon^2)$, υ is poison ratio, E is Young's modulus, and G is the shear modulus.

4. The compatibility equation

$$\nabla^2(\sigma_{xx} + \sigma_{yy}) = 0. \tag{4}$$

Where ∇^2 is Laplace operator. This equation guarantees the single valudness of the displacement vector ($Q=[u\ v]^t$), and the continuity of the solution to the stress field inside the solid.

It is theoretically proven that stress and shear can be

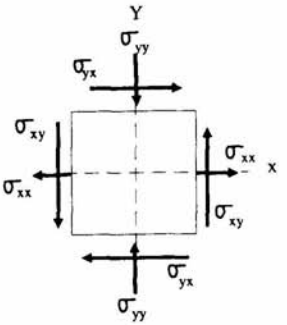

Figure 2a: An infinitesmal element inside the solid.

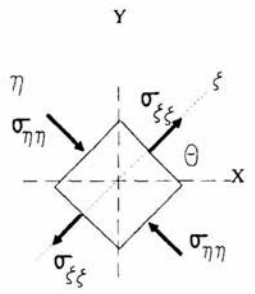

Figure 2b: The element along the principle axis.

written as

$$\sigma_{xx} = \frac{\partial^2 F(x,y)}{\partial y^2}, \quad \sigma_{yy} = \frac{\partial^2 F(x,y)}{\partial x^2}, \quad \sigma_{xy} = \frac{\partial^2 F(x,y)}{\partial x\partial y} \tag{5}$$

F(x,y) is called the Airy stress function for simply connected regions. Substituting the above in the compatibility equation we have

$$\nabla^2\left(\frac{\partial^2 F(x,y)}{\partial x^2} + \frac{\partial^2 F(x,y)}{\partial y^2}\right) = 0$$
$$\nabla^2\nabla^2(F(x,y)) = 0 \tag{6}$$
$$\nabla^4 F(x,y) = 0.$$

As can be seen the Airy stress function is in fact the Biharmonic potential function. It has been shown that solving the above equation given the value of the stress on the boundary of the object can be used to compute the stress every where in the object.

Potential Field Generation

Consider a 2-D slap of a homogeneous solid. Assume that cavities are created in the solid that have a boundary Γ that coincide with that of the obstacles (Figure-3). Also, assume that a tiny pressurized bubble of boundary β exist at the target. As will be shown in the sequel a pressure field that is usable for navigation will emanate from the bubble and span the whole inside of the solid (Ω). The resulting BVP is

solve $\quad \nabla^4 F(x,y) = 0$

subject to

$$\frac{\partial^2 F(x,y)}{\partial x^2}\Big|_{\beta} = P\cdot n\beta_y, \quad \frac{\partial^2 F(x,y)}{\partial y^2}\Big|_{\beta} = P\cdot n\beta_x, \quad \frac{\partial^2 F(x,y)}{\partial x\partial y}\Big|_{\beta} = 0.$$

$$\frac{\partial^2 F(x,y)}{\partial x^2}\Big|_{\Gamma} = \frac{\partial^2 F(x,y)}{\partial y^2}\Big|_{\Gamma} = \frac{\partial^2 F(x,y)}{\partial x\partial y}\Big|_{\Gamma} = 0. \tag{7}$$

The pressure inside β (P) can be controlled to make the deformation of Γ negligible. However, any deformation can be eliminated by applying fixed mechanical supports at Γ (i.e. no rotation or translation are allowed). For such a case, both the stress on β and the displacement on Γ are specified. The corresponding BVP becomes: Jointly solve the biharmonic equation

$$\nabla^4 F(x,y) = 0$$

and Hook's Law

$$(\nabla F)(\nabla F)^t = \lambda[\nabla\cdot Q(x,y)]I + G[J(Q(x,y)) + J^t(Q(x,y))].$$

subject to

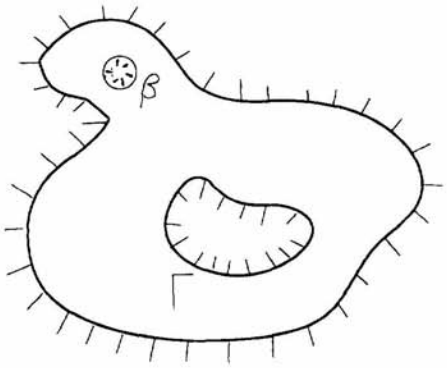

Figure 3: Regions in the soild.

$$\left.\frac{\partial^2 F(x,y)}{\partial x^2}\right|_{\beta} = P\cdot n\beta_y, \quad \left.\frac{\partial^2 F(x,y)}{\partial y^2}\right|_{\beta} = P\cdot n\beta_x, \quad \left.\frac{\partial^2 F(x,y)}{\partial x \partial y}\right|_{\beta} = 0.$$

and $\quad Q|_{\Gamma} = 0 \quad$ and $\quad \nabla x Q|_{\Gamma} = 0. \qquad (8)$

where $n\beta_x$ and $n\beta_y$ are the x and y components of the unit normal vector to β, I is the identity matrix, and $J(\ )$ is the Jacobian matrix.

The Tracking Mechanism

After the computation of the potential field comes the task of constructing the navigation field. Such a field is derived from the stress and shear components which can be computed from F using equation-5. We shall begin by examining the nature of the stress lines that emanate from the pressurized bubble. Pressure can only apply normal stress to a surface (i.e. the shear component is zero). To track such stress lines in the material, the principal stresses ($\sigma_{\xi\xi}$, $\sigma_{\eta\eta}$) have to be computed. In order to do so, the infinitesimal elements inside the material have to be rotated (Figure-2b) such that the shear component in the new coordinates (principal coordinates) vanish ($\sigma_{\xi\eta}$). Finding these stresses is equivalent to finding the eigen values of the matrix

$$\Sigma = \begin{bmatrix} \sigma_{xx} & \sigma_{xy} \\ \sigma_{yx} & \sigma_{yy} \end{bmatrix}, \quad \text{such that} \quad \begin{bmatrix} \sigma_{\xi\xi} & 0 \\ 0 & \sigma_{\eta\eta} \end{bmatrix} = T^t \Sigma\, T. \qquad (9)$$

Where T is an orthonormal matrix that contains the eigen vectors which are the axis of the new principal coordinates. The principal stresses are used to construct two distinctive orthogonal stress fields: The maximum principal stress field (σ_{max}), and the minimum principal stress field (σ_{min})

$$\sigma_{max} = \max(\sigma_{\xi\xi}, \sigma_{\eta\eta}) \qquad \sigma_{min} = \min(\sigma_{\xi\xi}, \sigma_{\eta\eta})$$

Those fields can be directly computed from the stress and shear components along the X and Y axis using the formulae

$$\sigma_{max} = \frac{\sigma_{xx} + \sigma_{yy}}{2} + \sqrt{\frac{\sigma_{xx} + \sigma_{yy}}{2} + \sigma_{xy}^2}$$

$$\sigma_{min} = \frac{\sigma_{xx} + \sigma_{yy}}{2} - \sqrt{\frac{\sigma_{xx} + \sigma_{yy}}{2} + \sigma_{xy}^2}$$

The angles along which these stresses are pointing is computed by solving

$$\theta = \frac{1}{2}\ \mathrm{atan}\left(-\frac{\sigma_{xx} - \sigma_{yy}}{2\sigma_{xy}}\right).$$

The above equation has two solutions θ_1 and θ_2 from which the angles of the principal stresses can be computed as

$$\theta_{max} = \min(|\theta_1|, |\theta_2|), \qquad \theta_{min} = \max(|\theta_1|, |\theta_2|).$$

Since pressure causes compression which gives stress a negative value, and because there are no other sources of stress besides the bubble, the minimum principle stress lines are used to track the propagation of the stress lines that emanate from β. Since the continuity of the stress lines in Ω have been guaranteed by the compatibility equation (equation-4), a stress line emanating from β has to terminate on Γ, or loop back to β. A stress line can not discontinue its path inside Ω. Such a behavior is thoroughly discussed in [13]. As can be seen traversing these lines starting from any where in Ω will lead to the target. However the matter of in which direction to proceed needs to be decided. Although such a dilemma can be resolved by proceeding in the direction that leads to an increase in the magnitude of the stress, it is possible that such an approach may lead to numerical difficulties similar to those faced by the harmonic approach. This is expected to occur in areas far from the source where the differential in the magnitude of the stress is minute. To eliminate the potential for such a problem the following approach is adopted. We shall proceed under the assumption that the path to the target has to be compiled first then downloaded to the robot for traversal. We shall traverse the field lines in both directions. This will result in two paths from which one is guaranteed to converge while the other may not converge. The path that leads to the target first is adopted and the other is discarded. The corresponding differential equations that generates these paths have the form

$$\dot{x}_+ = \alpha\cdot n\sigma_+(x,y), \quad \dot{x}_- = \alpha\cdot n\sigma_-(x,y).$$

Where $n\sigma_+(x,y)$ is a unit vector that drives motion in the forward direction, and $n\sigma_-(x,y)$ drives motion in the backward direction, and α is a positive constant.

IV RESULTS

In this section the proposed approach is simulated and the results are compared with those of the harmonic potential approach. The comparison is carried out with both the Dirichlet setting of the harmonic approach [6], which is known to severely suffer from a rapidly vanishing navigation field, and the Neumann setting of the approach [7,8,9] which was suggested to alleviate this problem. The simulation is carried out using the I-DEAS™ [14,15] finite element software. Different environments were chosen to illustrate the difference between the biharmonic and the harmonic approach in terms of the nature of the path generated by each, and the ability of the navigation field to propagate in the workspace.

Figure-4 depicts a simple environment with the obstacle taken as a rectangular slap. Figure-4a,b show the navigation field from the Dirichlet and the Neumann setting of the harmonic approach respectively. The fast decay of the field from the Dirichlet setting is obvious. Figure-c,d show the minimum and maximum principle stress fields respectively. As can be seen the two stresses are orthogonal to each other, and the navigation field created by the minimum principle stress retains a significant value every where in the space. In figure 4e different paths laid using the stress field method (solid lines) are shown with their counterparts from the Neumann-set harmonic method (the

broken lines). As can be seen the path generated from the stress field experience less fluctuations and has a lower maximum absolute curvature than the one from the harmonic method. Figure-5 show a more realistic environment. Figure-5a,b show the navigation field from the harmonic approach, the Dirichlet setting and Neumann setting respectively. As can be seen in this case even the Neumann setting of the harmonic approach experience difficulties in the areas that are far from the target. However, the navigation field created by the biharmonic potential (Figure-5c) remain well-behaved all over the space. Figure-5d show different paths generated by the biharmonic method.

V. CONCLUSIONS

This paper suggests a new addition to the family of potential-based path planning techniques. The new approach utilizes the biharmonic potential and is shown to have a navigation field that retain significant value all over the workspace. This field is shown to be able to lay a well behaved, dynamically suitable for traversal path to the target. The paper also discusses a model for potential-based techniques that aim at explaining the success of such an approach in reducing the complexity of the navigation process which in turn makes a real-time implementation of a planner feasible. Our intention is to construct the model in a manner that would partition it into interconnected functionally distinct modules. The model that is suggested here is divided into two stages: A stage that is global in nature and function to communicate to every location in the space information that is relevant to achieving the objective. The second stage is local in nature and is concerned with utilizing this information to reach the goal. It is our believe that the ability to properly fan information to the space of interest combined with the proper linkage between micro action and macro behavior are the reason behind the success of the potential-based approach for navigation. As a last remark regarding the proposed approach for navigation we have to say that it is very interesting to know that a solid piece of material can be used to synthesize a form of goal-oriented intelligence.

REFERENCES

[1] Khatib O.,"Real-Time Obstacle Avoidance for Manipulators and Mobile Robots", The Int. Jour of Rob. Res., Vol.5, No.1,Spring 1986,pp 90-98.

[2] Pavlov V.,Voronin A.," The Method of Potential Functions for Coding Constraints of the External Space in an Intelligent Mobile Robot", Soviet Automatic Control, Vol.17, No.6, 1984, pp 45-51.

[3] Miyazaki,Arimoto S.,"Sensory Feedback Based on the Artificial Potential for Robots",Proc. of the 9'th IFAC, Budapest, Hungary, 1984.

[4] Masoud. A, Bayoumi M.," Constraining the Motion of a Robot Manipulator Using the Vector Potential Approach",1993 IEEE Regional Conf. on Aerospace Control Systems, Westlake Village,CA May 25-27, 1993,pp 493-497.

[5] Masoud. A, Bayoumi M.,"Robot Navigation Using the Vector Potential Approach", IEEE Int. Conf. on Rob. and Aut.,Atlanta Georgia, May 2-7, 1993 1:805-811.

[6] Connolly C., Weiss R., Burns J.,"Path Planning Using Laplace's Equation", IEEE Int. Conf. On Rob. and Aut. May 13-18, Cincinnati-Ohio, 1990 pp 2102-2106.

[7] Keymeulen D., Decuyper J.,"On the Self-Organizing Properties of Topological Maps",The First European Conf. on Artificial Life (ECAL91) Paris, Dec. 11-13, 1991.

[8] Decuyper J.,Keymeulen D.,"A Reactive Robot Navigation System Based on a Fluid Dynamics Metaphor", Parallel Proble Solving From Nature, 1st Workshop, PPSN1, Dortmund, FRG, OCT. 1-3, 1990. Proceedings.

[9] Blake A.,Tarassenko,"Analog Comoputation of Collision-free Paths",IEEE Int. conf. Rob. and Auto.,Sacramento California, Apr. 91,pp 2047-2053.

[10] Kim J.,Khosla P.,"Realtime Obstacle Avoidance Using Harmonic Potential Functions", IEEE Int. conf. Rob. and Auto.,Sacramento California, Apr. 91, pp 2047-2053.

[11] Shigley J.,"Mechanical Engineering Design",McGraw-Hill, first metric edition, 1986.

[12] Boresi A., Chong K.,"Elasticity in Engineering Mechanics", Elsevier, N.Y., Amesterdam, London, 1987.

[13] Frdrick D.,Chang T.,"Continuum Mechanics", scientific publishers inc, Boston, 1972.

[14] Lawry M.,"I-DEAS™: Student Guide", Structural Dynamics Research Corporation (SDRC), 1991.

[15] Grandin H. Jr.,"Fundamentals of the Finite Element Method", Macmillan Publishing Co., N.Y., 1986.

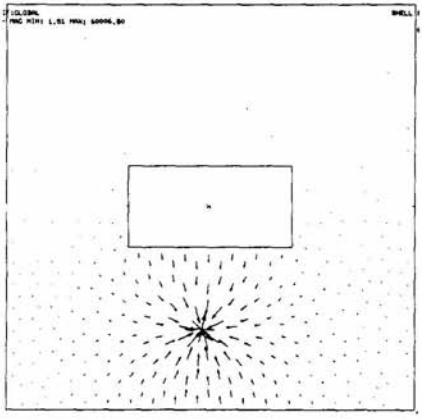

Figure-4a
The navigation field
Harmonic potential, Dirichlet setting.

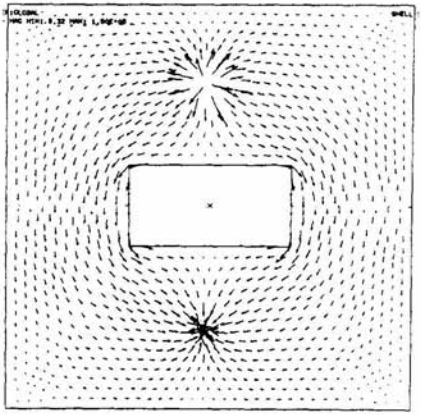

Figure-4b
The navigation field
Harmonic potential, Neumann setting.

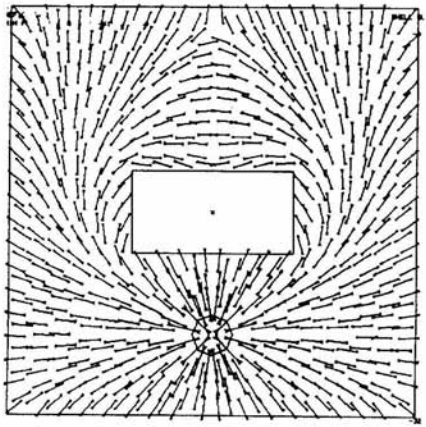

Figure-4c
The navigation field
Biharmonic potential, Minimum principle.

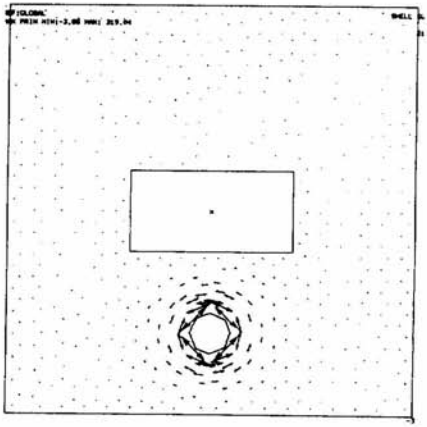

Figure-4d
Biharmonic potential, Maximum principle.

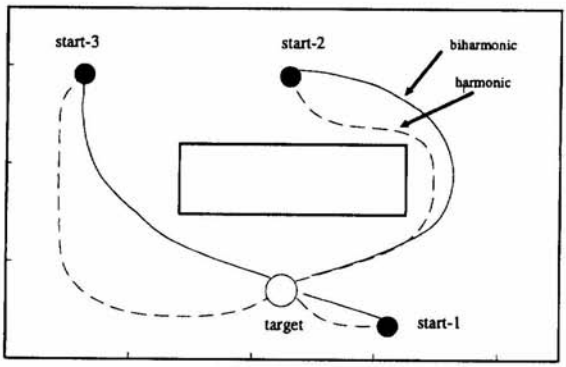

Figure-4e
Different paths to the target
Biharmonic - Solid lines.
Harmonic - Broken lines.

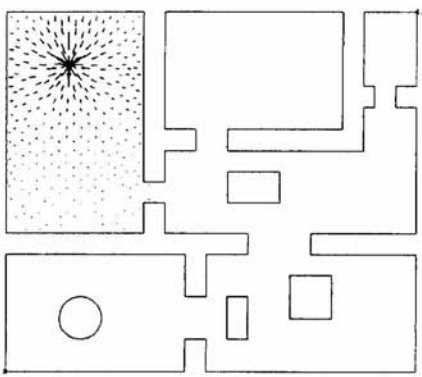

Figure-5a
The navigation field
Harmonic potential, Dirichlet setting.

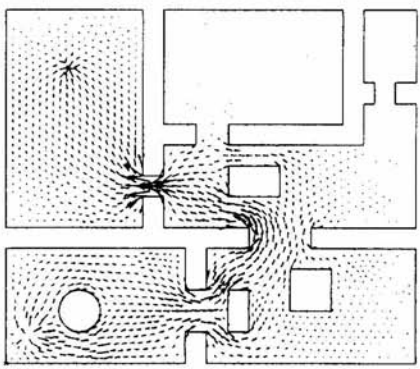

Figure-5b
The navigation field
Harmonic potential, Neumann setting.

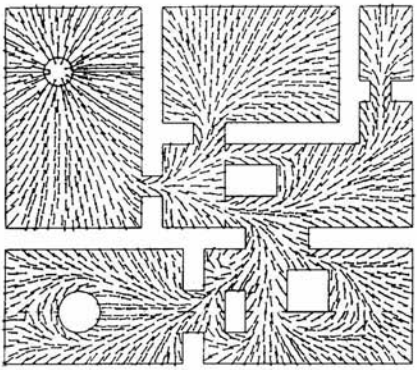

Figure-5c
The navigation field
Biharmonic potential, Minimum principle.

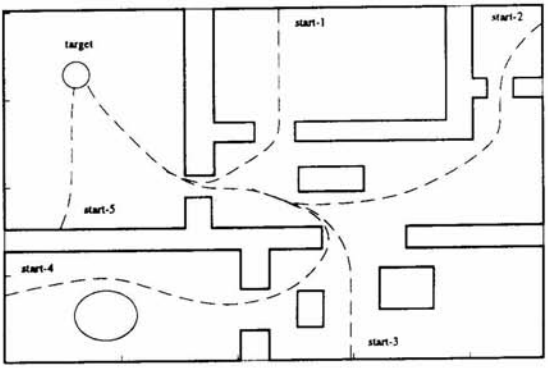

Figure-5d
Different paths to the target
The Biharmonic approach